HHS Public Access

Author manuscript

*Q J Nucl Med Mol Imaging*. Author manuscript; available in PMC 2021 March 23.

Published in final edited form as:

*Q J Nucl Med Mol Imaging*. 2020 March ; 64(1): 4–20. doi:10.23736/S1824-4785.20.03230-6.

# Current and Novel Radiopharmaceuticals for Imaging Cardiovascular Inflammation

**Gyu Seong Heo**, **Deborah Sultan**, **Yongjian Liu**

Mallinckrodt Institute of Radiology, Washington University, St. Louis, Missouri, 63110, United States

## Abstract

Cardiovascular disease (CVD) remains the leading cause of death worldwide despite advances in diagnostic technologies and treatment strategies. The underlying cause of most CVD is atherosclerosis, a chronic disease driven by inflammatory reactions. Atherosclerotic plaque rupture could cause arterial occlusion leading to ischemic tissue injuries such as myocardial infarction and stroke. Clinically, most imaging modalities are based on anatomy and provide limited information about the on-going molecular activities affecting the vulnerability of atherosclerotic lesion for risk stratification of patients. Thus, the ability to differentiate stable plaques from those that are vulnerable is an unmet clinical need. Of various imaging techniques, the radionuclide-based molecular imaging modalities including positron emission tomography (PET) and single-photon emission computerized tomography (SPECT) provide superior ability to noninvasively visualize molecular activities in vivo and may serve as a useful tool in tackling this challenge. Moreover, the well-established translational pathway of radiopharmaceuticals may also facilitate the translation of discoveries from benchtop to clinical investigation in contrast to other imaging modalities to fulfill the goal of precision medicine. The relationship between inflammation occurring within the plaque and its proneness to rupture has been well documented. Therefore, an active effort has been significantly devoted to develop radiopharmaceuticals specifically to measure CVD inflammatory status, and potentially elucidate those plaques which are prone to rupture. In the following review, molecular imaging of inflammatory biomarkers will be briefly discussed.

### Keywords

radiopharmaceuticals; imaging; cardiovascular; inflammation

## Introduction

In 2015, cardiovascular disease (CVD) was found responsible for one-third of overall deaths worldwide and is expected to account for >23.6 million deaths by 2030.[1–3] CVD comprises many conditions including heart disease, heart attack (myocardial infarction, MI), ischemic stroke, heart failure, arrhythmia, *etc*. The underlying cause of many CVD symptoms is

**Corresponding Author:** Yongjian Liu, Washington University School of Medicine, Department of Radiology, Campus Box 8225, 510 South Kingshighway Blvd, St. Louis, MO 63110-1016. Phone: 314-362-8431; Fax: 314-362-9940; yongjianliu@wustl.edu.

Conflict of interest

The authors confirm that this article content has no conflict of interest.

atherosclerosis. Influx of low-density lipoprotein (LDL) cholesterol from circulating blood to the arterial vessel wall initiates atherogenesis. It provokes the expression of endothelial cell adhesion molecules leading to leukocyte recruitment. The secretion of proinflammatory chemokines and cytokines from leukocytes triggers the innate and adaptive immune response leading to infiltration of additional circulating leukocytes. If the atherosclerotic lesions progress further, plaque rupture and potentially formation of thrombus could result, which, depending on the location of occlusion, could interrupt blood flow resulting in cerebral or myocardial ischemia. The major difficulty in managing atherosclerosis-driven CVD is timely detection of rupture-prone plaques while they are still asymptomatic. There are clinically available imaging techniques which can analyze atherosclerotic lesions including computed tomography (CT), magnetic resonance imaging (MRI), ultrasonography, and optical coherence tomography (OCT).[4] However, analysis of plaque morphology, such as extent of stenosis and thickness of fibrous cap, often fail to predict plaque rupture. Much scientific evidence indicates the critical role of inflammation throughout atherogenesis.[5] Notably, inflammation in the plaque is correlated with plaque instability.[6–8] Moreover, prognosis of atherosclerotic complications such as myocardial infarction are associated with inflammatory responses / recovery of injured tissue after such events. Biopsy, a procedure which is highly invasive and impractical for blood vessels and heart tissues, is the current method for detecting immune cells in lesions. Molecular imaging techniques such as positron emission tomography (PET) and single-photon emission computerized tomography (SPECT) can offer remarkable opportunities to resolve this critical issue due to their ability to non-invasively visualize the local expression and activity of inflammation-related molecules, cells, or functions that influence CVD progression, outcome, and/or responsiveness to therapeutics in individuals. $^{18}$F-FDG PET/CT has shown its capability to image inflammation in CVD, but has some limitations. Thus, there has been much effort to find more specific inflammation-related biomarkers and tools. In this review, we will discuss current and emerging targets for the imaging and treatment of CVD and radiopharmaceuticals that have been used in preclinical and clinical studies to examine CVD.

## Imaging cardiovascular inflammation using radiopharmaceuticals

Imaging cardiovascular inflammation presents a few unique challenges. On top of the small size of atherosclerotic lesions, their proximity to the blood pool often leads to poor imaging quality due to radiotracers in circulation. The complex pathophysiology of atherosclerotic plaques determines the low abundance and dynamic expression of disease-related targets on advanced plaques. Thus, the targeting specificity, sensitivity, pharmacokinetics of radiotracer, as well as appropriate imaging protocols are important to acquire optimal uptake and signal-to-background ratio for the accurate detection of plaques. Of the various imaging modalities, PET has been favored owing to its high sensitivity, quantitative and functional detection, non-invasive nature, and well-established pathways for human translation.[9, 10] Currently, most PET probes for atherosclerosis imaging are at preclinical stages, detecting specific cell surface markers during the progression of plaque, with few in clinical trials. Among the many types of inflammatory cells, monocytes and macrophages are particularly responsible for CVD development and progression.[5] Excessive macrophage content in atherosclerotic lesions is closely correlated with poor prognosis,[11] which makes it a popular

and logical choice as an imaging target for inflammation. Development of atherosclerosis is a multiple stages process including endothelial cell dysfunction and activation, inflammation, proteolysis and apoptosis, formation of lipid core and fibrous cap, angiogenesis, and thrombosis.[12] Each stage presents unique biomarker that can be detected via imaging approaches to provide us with key information in understanding the progress and status of disease. In this review, we only focus on the radiopharmaceuticals that can directly detect inflammatory cells, not the cause of inflammatory response (*e.g.* LDL deposition, expression of adhesion molecules on endothelial cells) or the results of inflammatory reaction (*e.g.* calcification, thrombosis).

**Glucose transporters (GLUTs)—**Enhanced glucose metabolism in activated inflammatory cells is the most widely studied marker for imaging inflammation. Inflammatory cells highly express glucose transporters, especially GLUT-1 and GLUT-3, but many cell types in the blood including monocytes, macrophages (M0, M1, and M2), neutrophils, natural killer cells, B cells, T cells, platelets, and endothelial cells also show overexpression of GLUT-1 and GLUT-3.[13] It has been demonstrated that the proinflammatory M1 macrophage has higher glycolytic activity due to the overexpression of glycolytic enzyme (hexokinase),[14] which leads to higher accumulation of metabolized glucose analogues (*e.g.* $^{18}$F-FDG) among other blood-derived cells.[15]

$^{18}$F-FDG PET is currently the primary tool for clinical PET imaging with a demonstrated capability of imaging inflammation in CVD. However, $^{18}$F-FDG uptake is not particularly specific to macrophages. Many other leukocytes and muscle cells, like cardiomyocytes and smooth muscle cells, also take up significant amounts of $^{18}$F-FDG leading to high background signal. Thus, detection of inflammation within tissues with high metabolic activity such as heart tissues and coronary arteries is challenging. Ischemia and hypoxia are also known to cause overexpression of GLUTs, which needs to be considered for interpretation of PET images.[16] Furthermore, high blood glucose can hinder $^{18}$F-FDG uptake, which requires fasting before imaging and can affect the image quality of diabetic patients. Due to these limitations, development of more specific biomarkers and their molecular imaging methods is highly desirable. Since the application of $^{18}$F-FDG PET imaging for atherosclerosis and myocardial inflammation has been comprehensively reviewed by several groups, we will focus on other radiotracers which can image cardiovascular inflammation.

**Chemokine receptors—**Since chemokines and their receptors play crucial roles in both primary and secondary immune response by modulating leukocyte migration and homing, they are promising targets for imaging inflammatory diseases such as atherosclerosis and its complications. Thus far, it has been known that *ca.* 20 chemokine receptors (G protein-coupled seven-transmembrane signaling receptors) and 50 endogenous chemokines are involved in complex and dynamic interactions to regulate immune responses. As the functions of each chemokine-receptor axis have been progressively discovered, their importance as a target for molecular imaging and anti-inflammatory therapy has expanded.

**a. CXCR4:** The importance of CXCR4 as a biomarker of atherosclerosis is well-documented in both animal models and humans.[17] In atherosclerotic mouse models,

treatment with CXCR4 antagonist elicited increased neutrophil recruitment and plaque inflammation resulting in larger atherosclerotic lesions.[18] In the same study, treatment with an antibody for neutrophil depletion reduced atherogenesis, indicating the role of neutrophils in inflammation. Other studies reported conflicting roles of CXCR4-CXCL12 axis. Although vascular CXCR4 expression prevents atherosclerosis,[19] endothelial CXCL12 exacerbates plaque development.[20] In human carotid plaques, upregulation of CXCR4 and CXCL12 were reported and CXCR4 expressions were colocalized with macrophages, leukocytes, smooth muscle cells, and small neovessels as confirmed by immunohistochemistry,[21] which is the basis of CXCR4-targeted imaging strategies.

$^{68}$Ga-pentixafor is a radiolabeled cyclic pentapeptide which is an analog of CXCL12, initially developed for CXCR4-specific tumor imaging.[22] It has been examined as a PET radiotracer in clinical trials for cancer imaging. For imaging atherosclerosis, preclinical,[23] retrospective,[24, 25] and clinical studies[26, 27] demonstrated that CXCR4 specific uptake of $^{68}$Ga-pentixafor was correlated with calcified plaque burden, extent of carotid stenosis, and cardiovascular risk factors, suggesting its potential for further evaluation of vulnerable atherosclerotic lesions. These studies also demonstrated CXCR4 upregulation within the plaques of rabbit and human, which was mainly colocalized with macrophage staining by immunohistochemistry.

Minimal myocardial uptake of $^{68}$Ga-pentixafor is a great advantage over $^{18}$F-FDG. In a myocardial infarction mouse model, an elevated uptake of $^{68}$Ga-pentixafor within the infarcted lesion was greatest at 3 days post MI, which was correlated with amount of CD45+ leukocytes measured by flow cytometry.[28] In addition, $^{68}$Ga-pentixafor PET imaging in post MI patients showed individual differences in radiotracer uptake indicating various degrees of inflammatory responses. Although further studies are needed, heart failure after myocardial infarction might be predicted based on $^{68}$Ga-pentixafor uptake, which is associated with the extent of CXCR4-related inflammatory reaction. Also, it might enable proper patient selection for immunomodulatory therapy. In a different study, $^{68}$Ga-pentixafor PET/CT showed potential to detect a culprit plaque within the coronary arteries of recent MI patients based on SUV.[26]

It is necessary to be cautious with interpretation of CXCR4 expression measured by $^{68}$Ga-pentixafor since it might provide mixed information from both beneficial CXCR4 signal from arterial endothelial cells or SMCs and detrimental CXCR4 signal from inflammatory cells within the plaques.[19] Moreover, the CXCR4-CXCL12 axis is involved in other important activities including hematopoiesis, angiogenesis, and organ development. Targeted therapy by modulating the CXCR4-CXCL12 axis will need to be well studied and planned.

**b. CCR2:** The CCR2-CCL2 axis is a well-known contributor during the initial stages of atherogenesis, as it participates in the recruitment of CCR2+ inflammatory monocytes to the lesions.[17] The recruitment of CCR2+ monocyte/macrophage subset to the heart with ischemic injury was correlated to the adverse remodeling as a therapeutic target.[29] CCR2$^{-/-}$ mice show less monocytosis, leading to reduced atherogenesis. In addition, several CCR2 antagonists have been developed and demonstrated their efficacy, including an anti-CCR2

monoclonal antibody MLN1202 which is currently being evaluated in clinical trials. Therefore, molecular imaging of CCR2 has implications for both diagnosis and treatment.

ECL1i is a seven amino acid linear peptide which binds to the allosteric position in CCR2. $^{64}$Cu-radiolabeled ECL1i ($^{64}$Cu-DOTA-ECL1i) has been used for PET imaging of CCR2+ leukocytes in multiple animal models of inflammation, demonstrating its specificity to CCR2,[30, 31] and is currently being investigated in clinical trials for imaging lung inflammation and pancreatic cancer. This radiotracer has also been utilized for imaging cardiovascular inflammation. PET imaging of $^{64}$Cu-DOTA-ECL1i in an atherosclerotic Ldlr $^{-/-}$ mouse model with animals housed at different temperatures demonstrated higher tracer accumulation in the aortic arch of mice kept at lower temperatures, which was correlated with plaque macrophage content.[32] PET imaging of the same tracer in a mouse model of atherosclerotic plaque regression showed that levels of CCR2+ monocytes and macrophages decreased over time, indicating the contribution of inflammatory leukocyte emigration to plaque regression.[33] In addition, $^{68}$Ga-radiolabeled ECL1i ($^{68}$Ga-DOTA-ECL1i) was capable of imaging CCR2+ leukocytes in vivo (Figure 1).[34] In two independent mouse models of sterile cardiac injury, $^{68}$Ga-DOTA-ECL1i demonstrated significant uptake in the lesion which was associated with CCR2+ monocyte/macrophage content. $^{68}$Ga-DOTA-ECL1i showed minimal myocardial uptake which could provide higher signal-to-background ratio for imaging the coronary artery. Since it is known that cardiac resident non-inflammatory macrophages do not express CCR2, PET imaging with radiolabeled ECL1i could detect/quantify particularly inflammatory subset, CCR2+ macrophage and monocytes, which can reveal monocyte/macrophage dynamics at the systemic level.[35] Individual differences in CCR2+ immune cell contents in the lesions can guide CCR2-targeted immunomodulatory therapy in the near future.

ECL1i-targeted $^{64}$Cu-doped gold nanoclusters ($^{64}$CuAuNCs-ECL1i) showed CCR2 specific binding in lung transplanted mice with ischemia-reperfusion injury, which can be further evaluated for imaging cardiovascular inflammation.[30] As nanoparticles can load and deliver therapeutics, they can be applied for a theranostic approach.

**c. CCR5:** Upregulation of CCR5 in monocytes, macrophages, and T lymphocytes is well-documented. Multiple studies have pointed out the important role of the CCR5-CCL5 axis in atherogenesis as CCR5 knock-out,[36] treatment with CCR5 antagonist maraviroc,[37] or CCL5 receptor antagonist Met-RANTES[38] result in the decreased formation of atherosclerotic lesions. Especially, maraviroc is already FDA-approved for HIV treatment which showed anti-atherogenic effect in small number of HIV-HCV patients.[39] CCR5 imaging will not only provide information on atherogenesis based on leukocyte recruitment, but also has potential to be an in vivo companion diagnostic method for treatment with CCR5 antagonists. CCR5-targeted PET imaging was reported using a small peptide CCR5 antagonist, D-Ala1-peptide T-amide (DAPTA). $^{64}$Cu-radiolabeled DAPTA peptide ($^{64}$Cu-DOTA-DAPTA) and DAPTA-conjugated polymeric nanoparticles ($^{64}$Cu-DOTA-DAPTA-comb) were tested in a femoral artery wire injury model in apoE$^{-/-}$ mice. Although both tracers demonstrated higher uptakes in injured lesions than in sham-operated arteries, the nanoparticle-based radiotracer showed higher accumulation.[40] Recently, CCR5-specific

binding of $^{111}$In-DOTA-DAPTA was tested by an in vitro cell binding assay and ex vivo autoradiography studies in apoE$^{-/-}$ mice showing its potential as a SPECT radiotracer.[41]

**d. Broad spectrum chemokine receptor targeting ligand:** Viral macrophage inflammatory protein II (vMIP-II) is a chemokine receptor antagonist which shows high affinity to multiple chemokine receptors, including CCR1, CCR2, CCR3, CCR5, CCR8, CCR10, CXCR4, CX3CR1, and XCR1.[42, 43] Using this protein, multiple chemokine receptor targeting probes were developed which might enable a more comprehensive assessment of chemokine receptors involved in atherosclerosis. PET imaging of $^{64}$Cu-DOTA-vMIP-II in a wire-injury apoE$^{-/-}$ mouse model and in vivo competitive receptor blocking studies demonstrated at least 8 chemokine receptors contribute to the uptake, including CCR1, CCR2, CCR3, CCR4, CCR5, CCR8, CXCR4, and CX3CR1.[44] A polymeric nanoparticle-based approach was evaluated, showing higher accumulation of $^{64}$Cu-vMIP-II-Comb at the injury site due to the longer in vivo availability of nanoparticle-based radiotracer and the multivalent interactions between the targeted nanoparticles and their receptors.[45] However, more studies are required to understand contribution of each chemokine receptor to the PET signal for better interpretation of imaging results.

**Somatostatin receptor subtype-2 (SST2 or SSTR-2)—**SSTR2 is upregulated as monocytes differentiate into activated macrophages. Reverse transcription polymerase chain reaction (RT-PCR) and RNA sequencing data showed SSTR2 is highly expressed in proinflammatory M1 macrophages compared to other blood-derived cells including monocytes, macrophages (M0 and M2), neutrophils, natural killer cells, B cells, T cells, platelets, and endothelial cells.[13, 46] Notably, the low SSTR2 expression on unstimulated M0 macrophages and M2 macrophages could make SSTR2 an ideal biomarker to image inflammation.

Radiolabeled somatostatin analogues were developed for imaging and radionuclide therapy of neuroendocrine tumors having overexpressed SSTR. Preclinical studies have demonstrated SSTR2-specific binding of $^{68}$Ga-DOTATATE and $^{68}$Ga-DOTANOC to macrophages within the atherosclerotic plaques in the mouse aorta.[47, 48] Retrospective clinical studies have shown that PET imaging of oncology patients with radiopeptides, including $^{68}$Ga-DOTATATE and $^{64}$Cu-DOTATATE, demonstrated increased uptakes in both coronary arteries[49, 50] and large arteries,[51] and correlated radiotracer uptake with cardiovascular risk factors. One study claimed $^{64}$Cu-DOTATATE showed higher uptake in large arteries and better correlation with risk factors than $^{68}$Ga-DOTATOC.[52] Another clinical study reported $^{68}$Ga-DOTATOC PET/CT showed higher uptake in the infarcted or inflamed lesions of myocardium in patients of peri-/myocarditis or sub-acute myocardial infarction. Additional studies will be needed to compare these radioligand derivatives and select the appropriate radionuclides and targeting peptides for further imaging. One interesting finding was that $^{68}$Ga-DOTATATE and $^{18}$F-FDG uptakes were not colocalized in many cases, which suggests these two tracers bind to different cell populations.[51]

More systemic clinical studies were conducted in the patients with CVD. $^{64}$Cu-DOTATATE PET/MRI images in patients with stroke or transient ischemic attack were performed before carotid endarterectomy showing higher uptake in plaques.[53] Subsequent

immunohistochemical analysis of collected plaque specimens showed overexpression of CD68 (marker of M1 macrophage) and CD163 (marker of M2 macrophage). Surprisingly, in the same study, gene expression analysis by RT-PCR and multivariate analysis found that SUV was the only correlation with CD163 expression, which was contrary to other reports. Further confirmation studies are required to support this claim. More comprehensive clinical study was performed with $^{68}$Ga-DOTATATE PET/CT in CVD patients (Figure 2).[13] The mean of maximum tissue-to-blood ratios ($mTBR_{max}$) of $^{68}$Ga-DOTATATE measured from clinical images were well correlated with SSTR2 and CD68 gene expression as well as with autoradiography and immunohistochemistry studies of explanted carotid samples, which suggests SSTR2 overexpressed M1 macrophage-driven uptake within the plaques. They also showed both $^{68}$Ga-DOTATATE and $^{18}$F-FDG are capable of differentiating culprit vs. nonculprit carotid arteries and high- vs. low-risk coronary arteries. However, due to much lower background myocardial uptake of $^{68}$Ga-DOTATATE than that of $^{18}$F-FDG, $^{68}$Ga-DOTATATE can be a better option for imaging atherosclerotic complications involving coronary vessels.

One interesting retrospective study was reported on the potential of radionuclide therapy with the beta-emitter $^{177}$Lu-DOTATATE (LUTATHERA®), an FDA approved treatment of gastroenteropancreatic neuroendocrine tumors.[54] An analysis of oncology patients who received radionuclide therapy revealed that $^{177}$Lu-DOTATATE treatment reduced $^{68}$Ga-DOTATATE accumulation in plaques, suggesting radionuclide therapy affected the inflammatory states within the plaque. Although no histological confirmation was provided, further studies are warranted to explore radionuclide therapy as a theranostic treatment option for atherosclerosis.

**Mitochondrial membrane translocator protein (TSPO)—**TSPO is also known as peripheral benzodiazepine receptor (PBR). Although TSPO's function is not fully understood, its upregulation in inflammatory lesions is well documented, especially in association with neuroinflammation[55] and the cardiovascular system.[56] A light sheet fluorescence microscopy study of apoE$^{-/-}$ mouse descending aortas demonstrated colocalization of TSPO signal with CD11b+ monocyte-derived infiltrating macrophages but not with F4/80+ tissue resident macrophages, indicating TSPO's potential to selectively detect subpopulations of macrophages in atherosclerotic lesions.[57] Due to the overexpression of TSPO in activated microglia, several radiotracers have already been developed for imaging neuroinflammatory diseases.[58] Since a TSPO antagonist, PK11195 has been radiolabeled and the most widely used radiotracer for imaging neuroinflammation, it was the first tested for atherosclerosis imaging. In vitro autoradiography, immunohistochemistry studies, and confocal fluorescence microscopy showed colocalization of radiolabeled PK11195 signals and macrophage staining in human carotid endarterectomy specimens, demonstrating the feasibility of PK11195 for imaging atherosclerosis.[59, 60] PET/CT imaging of $^{11}$C-PK11195 in carotid stenosis patients showed its potential to detect inflammatory macrophages in an atherosclerotic plaque.[61] In addition, several next generation TSPO-targeted radioligands have been developed to improve the specificity and signal-to-noise ratio for imaging neuroinflammation, which can then be carried over to imaging cardiovascular inflammation.[58, 62] Outside of radiolabeled PK11195,

$^{18}$F-FEDAA1106,[63] $^{18}$F-FEMPA,[64] and $^{18}$F-GE180[65] have been tested but showed mixed results. For example, ex vivo autoradiography of $^{18}$F-FEMPA in the mouse aorta showed uptake colocalized with macrophage and TSPO expression by IHC. However, its uptake in the aorta measured by PET/CT was comparable to that in normal vessel wall. Since these tracers were originally developed for neuroimaging, they can pass the blood-brain barrier, offering a unique opportunity for whole body imaging that can monitor the inflammatory responses within both the cardiovascular systems and the brain. The influence of systemic inflammation triggered by myocardial infarction on a brain was investigated in addition to monitoring cardiac inflammation by single whole body PET imaging of $^{18}$F-GE180.[65] As shown in the same study, TSPO imaging might also detect mitochondrial dysfunction that is not directly related to the inflammation. An inherent limitation of TSPO-targeted radiotracers is difficulty in heart imaging due to a high cardiac mitochondrial content contributing high background uptakes.

**Mannose receptor or macrophage mannose receptor (MMR)—**In high risk atherosclerotic lesions with neovasculization and hemorrhage, upregulation of MMR on alternatively activated (M2) macrophages has been reported.[66] A few MMR-targeted radiopharmaceuticals have been studied for cardiovascular imaging. $^{18}$F-radiolabeled mannose ($^{18}$F-FDM) was clearly the first choice. Although higher $^{18}$F-FDM uptake into macrophages was observed compared to $^{18}$F-FDG in vitro, in vivo and ex vivo studies showed both $^{18}$F-FDM and $^{18}$F-FDG having similar uptakes in atherosclerotic rabbits.[67] Since mannose is also known to be taken up by macrophages through GLUTs as an epimer of glucose, $^{18}$F-FDM uptake has to be a sum of uptake via GLUTs and MMR, which might report additional information compared to $^{18}$F-FDG. However, it means they also shares limitations of $^{18}$F-FDG PET imaging. In order to improve specificity to MMR, mannose was conjugated to serum albumin, which prevents uptake through GLUTs as a result of its bigger size.[68] The resulting $^{68}$Ga-NOTA-neomannosylated human serum albumin ($^{68}$Ga-NOTA-MSA) showed higher SUVs in abdominal aortas of atherosclerotic rabbits than that of $^{18}$F-FDG, which might suggest an involvement of phagocytic activity due to the nanometer size of MSA. Radiolabeling MSA with longer-lived radionuclides will enable biodistribution at later time points to collect the pharmacokinetic information to broaden its potential application. Recently, a $^{68}$Ga-labeled MMR single-domain antibody, or nanobody, was examined in atherosclerotic mouse and rabbit models and exhibited higher accumulation in aortas compared to healthy control groups.[69] Interestingly, in the same study, uptakes of $^{68}$Ga-MMR, $^{18}$F-FDG, and $^{18}$F-NaF were not colocalized, demonstrating the involvement of different inflammatory cell populations and/or uptake mechanisms. While more rigorous studies are required to verify underlying uptake mechanisms, the study pointed out the potentially complementary role of each tracer. The FDA approved $^{99m}$Tc-tilmanocept, used clinically for imaging lymph nodes, is a mannose- and DTPA chelator-conjugated dextran that can be radiolabeled with various other radiometals. $^{111}$In-tilmanocept SPECT/CT was assessed in apoE$^{-/-}$ mice and demonstrated MMR-specific accumulation in aortic plaques.[70] Radiolabeling mannose-conjugated dextrans with PET radionuclides will be required to improve imaging quality. However, a major limitation of MMR-related preclinical studies is the lack of an adequate animal model that overexpress MMR, making it difficult to do comparative studies with other radioligands.

**Macrophage proliferation - Choline transporters—**Active and proliferating cells, including tumor cells and activated macrophages, have high cellular membrane turnover rates. Thus, monitoring cell membrane biosynthesis is an interesting option for tracking inflammation. Choline is a precursor for phosphatidylcholine, a major component of cellular membranes. Radiolabeled choline can be internalized by inflammatory cells and metabolized to become a part of the cell membrane. Ex vivo autoradiography and IHC studies demonstrated higher accumulation and macrophage co-localization of $^{18}$F-fluorocholine ($^{18}$F-FCH or $^{18}$F-choline)[71] and $^{11}$C-choline[72] within the aortic plaques of an atherosclerotic mouse model. Clinically, cholines have been used for cancer imaging. Retrospective studies have been conducted to examine the feasibility of using radiolabeled cholines to image vessel walls with PET/CT. Researchers looked at the relationship between arterial choline uptake in a mouse diabetes model and saw that $^{18}$F-FMCH accumulation was higher in diabetic hypercholesterolemic mice than in non-diabetic mice, although their macrophage contents were comparable.[73] Although a reason for higher $^{18}$F-FMCH uptake in diabetic mice needs to be verified, this study showed the diagnostic potential for imaging choline transportation in patients with type 2 diabetes mellitus, an advantage since interpretation of $^{18}$F-FDG imaging is complicated due to the elevated blood glucose levels of these patients. A recent clinical trial revealed that $^{18}$F-FCH PET/CT in stroke patients (n = 10) showed higher uptake in carotid plaques, which were not correlated with severity of carotid stenosis but closely correlated with macrophage contents and patient symptoms (Figure 3).[74] This study demonstrated the potential of $^{18}$F-FCH PET imaging to differentiate vulnerable plaques from stable ones.

Another recent study examined choline uptake and its subsequent metabolism in inflammatory reactions, finding a correlation between upregulation of the choline transporter-like protein-1 (CTL1) on activated macrophages and increased choline uptake.[75] In addition, inhibition of choline uptake or its metabolism reduced inflammasome activation and release of cytokines such as IL-1β and IL-18. More importantly, this study showed treatment with choline kinase inhibitor in two mouse models of acute inflammation ameliorated IL-1β-dependent inflammation. Although their side effects are not evaluated yet, choline transporter and choline metabolism will be promising targets upon which to develop novel treatment strategies. Therefore, related molecular imaging techniques will be of great importance as well.

**Macrophage proliferation – Nucleotide salvage pathway—**Rapidly proliferating cells such as tumor cells show an accelerated cell cycle including faster DNA synthesis. Since activated macrophages are known to have similar proliferation rates to tumor cells,[76] the cell cycle is an attractive target for macrophage imaging. DNA replication requires nucleotides as building blocks. The accumulation of $^{18}$F-radiolabeled thymidine analog ($^{18}$F-FLT) in proliferating cells by the thymidine salvage pathway and subsequent phosphorylation has been used for PET imaging of tumors. $^{18}$F-FLT PET imaging also showed higher uptakes in plaques of atherosclerotic mice, rabbits, and humans without significant myocardial uptakes compared to $^{18}$F-FDG (Figure 4).[77] However, uptakes in other proliferating cells including parenchymal cells deteriorate specificity of $^{18}$F-FLT since endothelial and smooth muscle cells also consist of plaques. In addition, the contribution of

de novo thymidine synthesis to proliferation of macrophage subsets needs to be studied and considered as its influence on tumor cells is already reported.[78] More preclinical and clinical studies are required to further assess its feasibility to image cardiovascular inflammation reliably.

**Phagocytic activity—**Nanoparticles are taken up by phagocytes as a part of the host defense. There are a variety of phagocytic cells including monocytes, macrophages, neutrophils, lymphocytes, dendritic cells, Kupffer cells, and mast cells. Among them, macrophages play a major role in the phagocytosis of nanoparticles. This phagocytic activity of inflammatory macrophages within atherosclerotic plaques and/or injured myocardium makes them an attractive target for molecular imaging. $^{64}$Cu-radiolabeled/fluorophore-tagged dextranated iron oxide nanoparticles ($^{64}$Cu-TNP, d = 20 nm)[79] and $^{89}$Zr-radiolabeled/fluorophore-tagged dextran nanoparticles ($^{89}$Zr-DNP, d = 13 nm)[80] were reported as multimodality nanoparticle probes for imaging of inflammatory macrophages in atherosclerosis. Following administration of $^{64}$Cu-TNP or $^{89}$Zr-DNP in the apoE$^{-/-}$ mice, flow cytometry analysis of the aortas indicated that the majority of uptake was found in monocytes/macrophages (73.9% and 76.7%, respectively). Comparison of SUVs between $^{64}$Cu-TNP and $^{18}$F-FDG in the same apoE$^{-/-}$ mouse model showed comparable uptake, although SUV and target-to-background ratio of $^{64}$Cu-TNP was a little higher. The $^{89}$Zr-DNP radiotracer was able to monitor treatment efficacy following siRNA treatment to silence CCR2. In another study, $^{18}$F-radiolabeled renal clearable polyglucose nanoparticles ($^{18}$F-Macroflor, d = 5 nm) were developed for PET imaging (Figure 5).[81] Due to its rapid blood clearance (6.5 min in mice and 22.5 min in rabbits), the authors chose more clinically relevant $^{18}$F for radiolabeling. Comparison with $^{18}$F-FDG showed that $^{18}$F-Macroflor had comparable SUVs, but minimal myocardial uptake which is a favorable property for potential heart imaging applications. However, the major limitation of measuring $^{18}$F-Macroflor uptake purely on phagocytic activity is the same as $^{18}$F-FDG, non-specificity, since both inflammatory and non-inflammatory macrophages participate in nanoparticles uptake.

Nanoparticles have potential to provide interesting opportunities to improve both imaging and therapy. As described above, multiple imaging modalities can be incorporated into a single nanoparticle scaffold. Additional targeting ligands can be readily added into the same platform yielding multiple-targeting probes, leading to improved imaging qualities with more comprehensive information in one scan. Interpretation of targeting with ligand-decorated nanoparticles needs to be done carefully, since targeting ligand specific binding/uptake of nanoparticles is accompanied with baseline uptake of nanoparticles by phagocytes. In addition, extended blood circulation of nanoparticles results in high background signal in blood pool organs, which might compromise signal-to-background ratios. Most importantly, therapeutic agents can be loaded into or onto nanoparticles enabling theranostic approaches. However, short-term and long-term nanotoxicity concerns have to be addressed before clinical trials.

**Leukocyte (Lymphocyte) Function-associated Antigen-1 (LFA-1)—**Adhesion of leukocytes to the arterial endothelium and subsequent migration into the intima is the initial

event of atherogenesis. Most leukocytes, including monocytes, macrophages, neutrophils, lymphocytes, basophils, and eosinophils, express LFA-1 on their cell surface.[82] Interactions between LFA-1 and Intercellular Adhesion Molecule 1 (ICAM-1) lead to transmigration of LFA-1 expressing cells.[83] Immunohistochemistry revealed LFA-1-positive cells in atherosclerotic lesions of animal models, making LFA-1 an interesting biomarker for imaging inflammatory cells in cardiovascular diseases.[84]

Butylamino-NorBIRT is an LFA-1 antagonist; DOTA-conjugated butylamino-NorBIRT (DANBIRT) was developed for SPECT and PET imaging after radiolabeling with various radiometals. SPECT/CT imaging demonstrated uptake of $^{111}$In-DANBIRT in the aortic arch of apoE$^{-/-}$ mice.[85, 86] Autoradiography and histological analysis in mouse and human specimens demonstrated $^{111}$In-DANBIRT uptake was colocalized with both LFA-1 expressing cells and CD68 positive macrophages, indicating specificity of this radiotracer to LFA-1. In addition, these studies showed minimal myocardial uptake of $^{111}$In-DANBIRT, an advantage over $^{18}$F-FDG. With the conjugation of the chelator DOTA in the DANBIRT, this precursor can be readily radiolabeled with various PET radionuclides such as $^{64}$Cu and $^{68}$Ga, thus expanding its applicability. Considering LFA-1 is expressed on most leukocytes, a contribution of each type of inflammatory cell to the PET signal is required to be studied. Although a broad spectrum DANBIRT imaging would provide comprehensive inflammatory response, a lack of specificity to each cell type might be a limitation.

## Other interesting biomarkers

**a. Interleukin-2 (IL-2) receptor:** IL-2 receptors are upregulated on activated T lymphocytes.[87] Thus, radiolabeled IL-2 might enable imaging of T cells in atherosclerotic plaques. $^{99m}$Tc-interleukin-2 ($^{99m}$Tc-IL2) scintigraphy was first tested for IL-2 receptor imaging in patients having carotid plaques. Results showed not only accumulation of the tracer in plaques but also correlation between tracer uptake and IL-2 receptor positive cells measured by immunohistochemistry and flow cytometry.[88] Patients who received statin treatment showed lower $^{99m}$Tc-IL2 uptake after treatment indicating its potential to monitor treatment response. In order to tackle the low resolution issue with $^{99m}$Tc-IL2, $^{18}$F-radiolabeled IL2 ($^{18}$F-FB-IL2) was developed.[89] PET imaging in activated human T-lymphocyte-inoculated SCID mice showed good correlation between inoculated cell numbers and $^{18}$F-FB-IL2 uptake. Further studies are required in atherosclerotic models to confirm its feasibility to detect activated T lymphocytes in vivo. Since the number of lymphocytes is less than macrophages, more sensitive radiotracer will be necessary to effectively detect them.

**b. Matrix metalloproteinases (MMPs):** Immune cells secrete or express a variety of chemicals including cytokines, chemokines, and enzymes, which promote inflammatory response. MMPs are a family of proteinases that play multiple roles in the inflammatory process.[90] They contribute to the atherosclerotic plaque rupture by participating in several processes including infiltration of immune cells, migration of smooth muscle cells to the fibrous cap, apoptosis, angiogenesis, and most importantly, degradation of the fibrous cap.[91] The major immune cells that release MMPs are macrophages. Thus, imaging MMPs would provide information on not a density of macrophages like most probes, but their activity to

promote inflammation and plaque rupture. As their names indicate, a metal ion, zinc is involved in the enzymatic activity of MMPs. Since all MMPs have similar zinc-binding motif that is only accessible in active forms, MMP inhibitors were designed to bind to the zinc ion as broad spectrum inhibitors. Some radiolabeled MMP inhibitors, such as $^{111}$In-DTPA-RP782 and $^{99m}$Tc-(HYNIC-RP805)(tricine)(TPPTS), have been examined for molecular imaging of CVD in multiple animal models including atherosclerosis, aneurysm, and vascular remodeling, which demonstrated their feasibility to monitor MMP activities.[91–94] As a distinct role of each subtype of MMPs has been revealed, however, the development of more selective inhibitors has been in progress to minimize side effects of treatment with broad spectrum inhibitors.[95, 96] Thus, there have been ongoing efforts to radiolabel next generation MMP inhibitors against MMP-2/9,[97] MMP-12,[98, 99] and MMP-13.[100] Thorough evaluation of next generation radioligands in multiple animal models is necessary.

## Conclusions and Perspectives

The importance of inflammation in cardiovascular diseases especially atherosclerosis has been well documented. Owing to the longitudinal nature of the inflammatory process and the complexity of diseases, many biomarkers have been identified, which has led to the development of numerous radiopharmaceuticals for cardiovascular inflammation imaging. These radiotracers not only significantly improved our understanding of the expression of specific biomarkers along the progression and regression of atherosclerosis, but also helped gaining insight about the role of inflammation in the pathogenesis of CVD to design treatment strategy.

Of the various imaging platforms, peptides and small molecules-based radiotracers have proven to be valuable tools for atherosclerosis detection due to the specificity and sensitivity. Although the fast in vivo pharmacokinetics and clearance may limit their applications to detect low abundance biomarkers, the low blood pool retention be useful to improve the target-to-background contrast ratio compared to other imaging agents with extended blood retention such as antibody and nanoparticles.

In contrast to well-established radiopharmaceuticals in oncology, there are still many challenges and issues to be addressed for the development of PET and SPECT tracers for cardiovascular diseases. It is critical to understand the dynamic roles of leukocytes and other pro- and anti-inflammatory mediators within atherosclerotic plaques in order to contain cardiovascular diseases. The integration of PET or SPECT imaging with the characterization of specific biomarker will improve our understanding of the complex biology of cardiovascular diseases. The dynamic variation of biomarkers at different stages of CVD may require the utilization of multiple radiotracers to fully characterize the progression and rupture potential of atherosclerosis. Particularly, how to interpret the rapid change of imaging data relative to the longitudinal transformation of plaque morphology is critical to assess the potential of radiotracer as a companion diagnostic for CVD.

Taken together, radionuclide-based molecular agents have been widely used for pre-clinical cardiovascular inflammation imaging. Although some radiotracers have been used for clinical investigations and showed promise to study human CVD biology, there is a long way

to go to propel the development of prognostic imaging agents not only to sensitively and specifically detect inflammatory biomarker for clinical translation, but also facilitate the advancement of precision cardiovascular medicine.

## Acknowledgements

This work is supported by 1R35HL145212-01 from NHLBI.

## References

1. Roth GA, Johnson C, Abajobir A, Abd-Allah F, Abera SF, Abyu G, et al. Global, Regional, and National Burden of Cardiovascular Diseases for 10 Causes, 1990 to 2015. J Am Coll Cardiol. 2017;70(1):1–25. [PubMed: 28527533]
2. Benjamin EJ, Muntner P, Alonso A, Bittencourt MS, Callaway CW, Carson AP, et al. Heart Disease and Stroke Statistics - 2019 Update: A Report From the American Heart Association. Circulation. 2019;139(10):e56–e528. [PubMed: 30700139]
3. Organization WH. Global status report on noncommunicable diseases 2014. World Health Organization, 2014.
4. Tarkin JM, Dweck MR, Evans NR, Takx RAP, Brown AJ, Tawakol A, et al. Imaging Atherosclerosis. Circ Res. 2016;118(4):750–69. [PubMed: 26892971]
5. Swirski FK, Nahrendorf M. Leukocyte Behavior in Atherosclerosis, Myocardial Infarction, and Heart Failure. Science. 2013;339(6116):161–6. [PubMed: 23307733]
6. Naghavi M, Libby P, Falk E, Casscells SW, Litovsky S, Rumberger J, et al. From Vulnerable Plaque to Vulnerable Patient. Circulation. 2003;108(14):1664–72. [PubMed: 14530185]
7. Libby P Inflammation in atherosclerosis. Nature. 2002;420(6917):868–74. [PubMed: 12490960]
8. Silvestre-Roig C, Winther MPd, Weber C, Daemen MJ, Lutgens E, Soehnlein O. Atherosclerotic Plaque Destabilization. Circ Res. 2014;114(1):214–26. [PubMed: 24385514]
9. LaForest R, Woodard PK, Gropler RJ. Cardiovascular PET/MRI: Challenges and Opportunities. Cardiol Clin. 2016;34(1):25–35. [PubMed: 26590777]
10. Amsallem M, Saito T, Tada Y, Dash R, McConnell MV. Magnetic Resonance Imaging and Positron Emission Tomography Approaches to Imaging Vascular and Cardiac Inflammation. Circ J. 2016;80(6):1269–77. [PubMed: 27151335]
11. Moore KJ, Sheedy FJ, Fisher EA. Macrophages in atherosclerosis: a dynamic balance. Nat Rev Immunol. 2013;13:709. [PubMed: 23995626]
12. Wu JC, Bengel FM, Gambhir SS. Cardiovascular Molecular Imaging. Radiology. 2007;244(2):337–55. [PubMed: 17592037]
13. Tarkin JM, Joshi FR, Evans NR, Chowdhury MM, Figg NL, Shah AV, et al. Detection of Atherosclerotic Inflammation by $^{68}$Ga-DOTATATE PET Compared to [$^{18}$F]FDG PET Imaging. J Am Coll Cardiol. 2017;69(14):1774–91. [PubMed: 28385306]
14. Pauwels EKJ, Sturm EJC, Bombardieri E, Cleton FJ, Stokkel MPM. Positron-emission tomography with [$^{18}$F]fluorodeoxyglucose. J Cancer Res Clin Oncol. 2000 9 01;126(10):549–59. [PubMed: 11043392]
15. Joseph P, Tawakol A. Imaging atherosclerosis with positron emission tomography. Eur Heart J. 2016;37(39):2974–80. [PubMed: 27125951]
16. Folco EJ, Sheikine Y, Rocha VZ, Christen T, Shvartz E, Sukhova GK, et al. Hypoxia But Not Inflammation Augments Glucose Uptake in Human Macrophages: Implications for Imaging Atherosclerosis With $^{18}$Fluorine-Labeled 2-Deoxy-D-Glucose Positron Emission Tomography. J Am Coll Cardiol. 2011;58(6):603–14. [PubMed: 21798423]
17. van der Vorst EPC, Peters LJF, Müller M, Gencer S, Yan Y, Weber C, et al. G-Protein Coupled Receptor Targeting on Myeloid Cells in Atherosclerosis. Front Pharmacol. 2019 2019-5-22;10(531). English.

18. Zernecke A, Bot I, Djalali-Talab Y, Shagdarsuren E, Bidzhekov K, Meiler S, et al. Protective Role of CXC Receptor 4/CXC Ligand 12 Unveils the Importance of Neutrophils in Atherosclerosis. Circ Res. 2008;102(2):209–17. [PubMed: 17991882]
19. Döring Y, Noels H, Vorst EPCvd, Neideck C, Egea V, Drechsler M, et al. Vascular CXCR4 Limits Atherosclerosis by Maintaining Arterial Integrity. Circulation. 2017;136(4):388–403. [PubMed: 28450349]
20. Döring Y, Vorst EPCvd, Duchene J, Jansen Y, Gencer S, Bidzhekov K, et al. CXCL12 Derived From Endothelial Cells Promotes Atherosclerosis to Drive Coronary Artery Disease. Circulation. 2019;139(10):1338–40. [PubMed: 30865486]
21. Merckelbach S, van der Vorst EPC, Kallmayer M, Rischpler C, Burgkart R, Döring Y, et al. Expression and Cellular Localization of CXCR4 and CXCL12 in Human Carotid Atherosclerotic Plaques. Thromb Haemost. 2018 //05.01.2018;118(01):195–206. En. [PubMed: 29304539]
22. Demmer O, Gourni E, Schumacher U, Kessler H, Wester H-J. PET Imaging of CXCR4 Receptors in Cancer by a New Optimized Ligand. ChemMedChem. 2011;6(10):1789–91. [PubMed: 21780290]
23. Hyafil F, Pelisek J, Laitinen I, Schottelius M, Mohring M, Döring Y, et al. Imaging the Cytokine Receptor CXCR4 in Atherosclerotic Plaques with the Radiotracer $^{68}$Ga-Pentixafor for PET. J Nucl Med. 2017 3 1, 2017;58(3):499–506. [PubMed: 27789718]
24. Weiberg D, Thackeray JT, Daum G, Sohns JM, Kropf S, Wester H-J, et al. Clinical Molecular Imaging of Chemokine Receptor CXCR4 Expression in Atherosclerotic Plaque Using $^{68}$Ga-Pentixafor PET: Correlation with Cardiovascular Risk Factors and Calcified Plaque Burden. J Nucl Med. 2018 2 1, 2018;59(2):266–72. [PubMed: 28775206]
25. Derlin T, Sedding DG, Dutzmann J, Haghikia A, Konig T, Napp LC, et al. Imaging of chemokine receptor CXCR4 expression in culprit and nonculprit coronary atherosclerotic plaque using motion-corrected [(68)Ga]pentixafor PET/CT. European journal of nuclear medicine and molecular imaging. 2018 10;45(11):1934–44. PubMed PMID: 29967943. Pubmed Central PMCID: PMC6132552. Epub 2018/07/04. eng. [PubMed: 29967943]
26. Derlin T, Sedding DG, Dutzmann J, Haghikia A, König T, Napp LC, et al. Imaging of chemokine receptor CXCR4 expression in culprit and nonculprit coronary atherosclerotic plaque using motion-corrected [$^{68}$Ga]pentixafor PET/CT. Eur J Nucl Med Mol Imaging. 2018 10 01;45(11):1934–44. [PubMed: 29967943]
27. Li X, Yu W, Wollenweber T, Lu X, Wei Y, Beitzke D, et al. [$^{68}$Ga]Pentixafor PET/MR imaging of chemokine receptor 4 expression in the human carotid artery. Eur J Nucl Med Mol Imaging. 2019 7 01;46(8):1616–25. [PubMed: 31004184]
28. Thackeray JT, Derlin T, Haghikia A, Napp LC, Wang Y, Ross TL, et al. Molecular Imaging of the Chemokine Receptor CXCR4 After Acute Myocardial Infarction. JACC: Cardiovascular Imaging. 2015 2015/12/01/;8(12):1417–26. [PubMed: 26577262]
29. Bajpai G, Bredemeyer A, Li W, Zaitsev K, Koenig AL, Lokshina I, et al. Tissue Resident CCR2- and CCR2+ Cardiac Macrophages Differentially Orchestrate Monocyte Recruitment and Fate Specification Following Myocardial Injury. Circ Res. 2019;124(2):263–78. [PubMed: 30582448]
30. Liu Y, Li W, Luehmann HP, Zhao Y, Detering L, Sultan DH, et al. Noninvasive Imaging of CCR2+ Cells in Ischemia-Reperfusion Injury After Lung Transplantation. Am J Transplant. 2016;16(10):3016–23. [PubMed: 27273836]
31. Liu Y, Gunsten SP, Sultan DH, Luehmann HP, Zhao Y, Blackwell TS, et al. PET-based Imaging of Chemokine Receptor 2 in Experimental and Disease-related Lung Inflammation. Radiology. 2017;283(3):758–68. PubMed PMID: 28045644. [PubMed: 28045644]
32. Williams JW, Elvington A, Ivanov S, Kessler S, Luehmann H, Baba O, et al. Thermoneutrality but Not UCP1 Deficiency Suppresses Monocyte Mobilization Into Blood. Circ Res. 2017;121(6):662–76. [PubMed: 28696252]
33. Li W, Luehmann HP, Hsiao H-M, Tanaka S, Higashikubo R, Gauthier JM, et al. Visualization of Monocytic Cells in Regressing Atherosclerotic Plaques by Intravital 2-Photon and Positron Emission Tomography-Based Imaging-Brief Report. Arter Thromb Vasc Biol. 2018;38(5):1030–6.

34. Heo GS, Kopecky B, Sultan D, Ou M, Feng G, Bajpai G, et al. Molecular Imaging Visualizes Recruitment of Inflammatory Monocytes and Macrophages to the Injured Heart. Circ Res. 2019;124(6):881–90. [PubMed: 30661445]
35. Fayad ZA, Swirski FK, Calcagno C, Robbins CS, Mulder W, Kovacic JC. Monocyte and Macrophage Dynamics in the Cardiovascular System: JACC Macrophage in CVD Series (Part 3). J Am Coll Cardiol. 2018 2018/10/30/;72(18):2198–212. [PubMed: 30360828]
36. Braunersreuther V, Zernecke A, Arnaud C, Liehn EA, Steffens S, Shagdarsuren E, et al. CCR5 But Not CCR1 Deficiency Reduces Development of Diet-Induced Atherosclerosis in Mice. Arter Thromb Vasc Biol. 2007;27(2):373–9.
37. Cipriani S, Francisci D, Mencarelli A, Renga B, Schiaroli E, D'Amore C, et al. Efficacy of the CCR5 Antagonist Maraviroc in Reducing Early, Ritonavir-Induced Atherogenesis and Advanced Plaque Progression in Mice. Circulation. 2013;127(21):2114–24. [PubMed: 23633271]
38. Veillard NR, Kwak B, Pelli G, Mulhaupt F, James RW, Proudfoot AEI, et al. Antagonism of RANTES Receptors Reduces Atherosclerotic Plaque Formation in Mice. Circ Res. 2004;94(2):253–61. [PubMed: 14656931]
39. Maggi P, Bruno G, Perilli F, Saracino A, Volpe A, Santoro C, et al. Effects of Therapy with Maraviroc on the Carotid Intima Media Thickness in HIV-1/HCV Co-infected Patients. In Vivo. 2017 1 1, 2017;31(1):125–31. [PubMed: 28064231]
40. Luehmann HP, Pressly ED, Detering L, Wang C, Pierce R, Woodard PK, et al. PET/CT Imaging of Chemokine Receptor CCR5 in Vascular Injury Model Using Targeted Nanoparticle. J Nucl Med. 2014 4 1, 2014;55(4):629–34. [PubMed: 24591489]
41. Wei L, Petryk J, Gaudet C, Kamkar M, Gan W, Duan Y, et al. Development of an inflammation imaging tracer, 111In-DOTA-DAPTA, targeting chemokine receptor CCR5 and preliminary evaluation in an ApoE−/− atherosclerosis mouse model. J Nucl Cardiol. 2019 8 01;26(4):1169–78. [PubMed: 29417414]
42. Kledal TN, Rosenkilde MM, Coulin F, Simmons G, Johnsen AH, Alouani S, et al. A Broad-Spectrum Chemokine Antagonist Encoded by Kaposi's Sarcoma-Associated Herpesvirus. Science. 1997;277(5332):1656–9. [PubMed: 9287217]
43. Szpakowska M, Chevigné A. vCCL2/vMIP-II, the viral master KEYmokine. J Leukoc Biol. 2016;99(6):893–900. [PubMed: 26701133]
44. Liu Y, Pierce R, Luehmann HP, Sharp TL, Welch MJ. PET Imaging of Chemokine Receptors in Vascular Injury–Accelerated Atherosclerosis. J Nucl Med. 2013 7 1, 2013;54(7):1135–41. [PubMed: 23658218]
45. Luehmann HP, Detering L, Fors BP, Pressly ED, Woodard PK, Randolph GJ, et al. PET/CT Imaging of Chemokine Receptors in Inflammatory Atherosclerosis Using Targeted Nanoparticles. J Nucl Med. 2016 7 1, 2016;57(7):1124–9. [PubMed: 26795285]
46. Dalm VA, van Hagen PM, van Koetsveld PM, Achilefu S, Houtsmuller AB, Pols DH, et al. Expression of somatostatin, cortistatin, and somatostatin receptors in human monocytes, macrophages, and dendritic cells. Am J Physiol Endocrinol Metab. 2003 8;285(2):E344–53. PubMed PMID: 12684217. Epub 2003/04/10. eng. [PubMed: 12684217]
47. Li X, Bauer W, Kreissl MC, Weirather J, Bauer E, Israel I, et al. Specific somatostatin receptor II expression in arterial plaque: $^{68}$Ga-DOTATATE autoradiographic, immunohistochemical and flow cytometric studies in apoE-deficient mice. Atherosclerosis. 2013 2013/9/01/;230(1):33–9. [PubMed: 23958249]
48. Rinne P, Hellberg S, Kiugel M, Virta J, Li X-G, Käkelä M, et al. Comparison of Somatostatin Receptor 2-Targeting PET Tracers in the Detection of Mouse Atherosclerotic Plaques. Mol Imaging Biol. 2016 2 01;18(1):99–108. [PubMed: 26122428]
49. Rominger A, Saam T, Vogl E, Übleis C, la Fougère C, Förster S, et al. In Vivo Imaging of Macrophage Activity in the Coronary Arteries Using $^{68}$Ga-DOTATATE PET/CT: Correlation with Coronary Calcium Burden and Risk Factors. J Nucl Med. 2010 2 1, 2010;51(2):193–7. [PubMed: 20080898]
50. Mojtahedi A, Alavi A, Thamake S, Amerinia R, Ranganathan D, Tworowska I, et al. Assessment of vulnerable atherosclerotic and fibrotic plaques in coronary arteries using $^{68}$Ga-DOTATATE

PET/CT. Am J Nucl Med Mol Imaging. 2014;5(1):65–71. PubMed PMID: 25625028. eng. [PubMed: 25625028]

51. Li X, Samnick S, Lapa C, Israel I, Buck AK, Kreissl MC, et al. 68Ga-DOTATATE PET/CT for the detection of inflammation of large arteries: correlation with 18F-FDG, calcium burden and risk factors. EJNMMI Res. 2012 2012/9/27;2(1):52. [PubMed: 23016793]
52. Malmberg C, Ripa RS, Johnbeck CB, Knigge U, Langer SW, Mortensen J, et al. $^{64}$Cu-DOTATATE for Noninvasive Assessment of Atherosclerosis in Large Arteries and Its Correlation with Risk Factors: Head-to-Head Comparison with $^{68}$Ga-DOTATOC in 60 Patients. J Nucl Med. 2015 12 1, 2015;56(12):1895–900. [PubMed: 26429961]
53. Pedersen SF, Sandholt BV, Keller SH, Hansen AE, Clemmensen AE, Sillesen H, et al. 64Cu-DOTATATE PET/MRI for Detection of Activated Macrophages in Carotid Atherosclerotic Plaques. Arter Thromb Vasc Biol. 2015;35(7):1696–703.
54. Schatka I, Wollenweber T, Haense C, Brunz F, Gratz KF, Bengel FM. Peptide Receptor–Targeted Radionuclide Therapy Alters Inflammation in Atherosclerotic Plaques. J Am Coll Cardiol. 2013 2013/12/17/;62(24):2344–5. [PubMed: 24076295]
55. Guilarte TR. TSPO in diverse CNS pathologies and psychiatric disease: A critical review and a way forward. Pharmacol Ther. 2019 2019/2/01/;194:44–58. [PubMed: 30189290]
56. Veenman L, Gavish M. The peripheral-type benzodiazepine receptor and the cardiovascular system. Implications for drug development. Pharmacol Ther. 2006 2006/6/01/;110(3):503–24. [PubMed: 16337685]
57. Kopecky C, Pandzic E, Parmar A, Szajer J, Lee V, Dupuy A, et al. Translocator protein localises to CD11b+ macrophages in atherosclerosis. Atherosclerosis. 2019 2019/5/01/;284:153–9. [PubMed: 30913515]
58. Vivash L, O'Brien TJ. Imaging Microglial Activation with TSPO PET: Lighting Up Neurologic Diseases? J Nucl Med. 2016 2 1, 2016;57(2):165–8. [PubMed: 26697963]
59. Fujimura Y, Hwang PM, Trout Iii H, Kozloff L, Imaizumi M, Innis RB, et al. Increased peripheral benzodiazepine receptors in arterial plaque of patients with atherosclerosis: An autoradiographic study with [$^{3}$H]PK 11195. Atherosclerosis. 2008 2008/11/01/;201(1):108–11. [PubMed: 18433754]
60. Bird JLE, Izquierdo-Garcia D, Davies JR, Rudd JHF, Probst KC, Figg N, et al. Evaluation of translocator protein quantification as a tool for characterising macrophage burden in human carotid atherosclerosis. Atherosclerosis. 2010 2010/6/01/;210(2):388–91. [PubMed: 20056222]
61. Gaemperli O, Shalhoub J, Owen DRJ, Lamare F, Johansson S, Fouladi N, et al. Imaging intraplaque inflammation in carotid atherosclerosis with $^{11}$C-PK11195 positron emission tomography/computed tomography. Eur Heart J. 2011;33(15):1902–10. [PubMed: 21933781]
62. Largeau B, Dupont A-C, Guilloteau D, Santiago-Ribeiro M-J, Arlicot N. TSPO PET Imaging: From Microglial Activation to Peripheral Sterile Inflammatory Diseases? Contrast Media Mol Imaging. 2017;2017:17.
63. Cuhlmann S, Gsell W, Van der Heiden K, Habib J, Tremoleda JL, Khalil M, et al. In Vivo Mapping of Vascular Inflammation Using the Translocator Protein Tracer 18F-FEDAA1106. Mol Imaging. 2014;13(6):7290.2014.00014.
64. Hellberg S, Silvola JMU, Kiugel M, Liljenbäck H, Savisto N, Li X-G, et al. 18-kDa translocator protein ligand $^{18}$F-FEMPA: Biodistribution and uptake into atherosclerotic plaques in mice. J Nucl Cardiol. 2017 6 01;24(3):862–71. [PubMed: 27225517]
65. Thackeray JT, Hupe HC, Wang Y, Bankstahl JP, Berding G, Ross TL, et al. Myocardial Inflammation Predicts Remodeling and Neuroinflammation After Myocardial Infarction. J Am Coll Cardiol. 2018 2018/1/23/;71(3):263–75. [PubMed: 29348018]
66. Gordon S Alternative activation of macrophages. Nat Rev Immunol. 2003 2003/1/01;3(1):23–35. [PubMed: 12511873]
67. Tahara N, Mukherjee J, de Haas HJ, Petrov AD, Tawakol A, Haider N, et al. 2-deoxy-2-[$^{18}$F]fluoro-d-mannose positron emission tomography imaging in atherosclerosis. Nat Med. 2014 01/12/online;20:215. [PubMed: 24412923]

68. Kim EJ, Kim S, Seo HS, Lee YJ, Eo JS, Jeong JM, et al. Novel PET Imaging of Atherosclerosis with $^{68}$Ga-Labeled NOTA-Neomannosylated Human Serum Albumin. J Nucl Med. 2016 11 1, 2016;57(11):1792–7. [PubMed: 27339872]
69. Senders ML, Hernot S, Carlucci G, van de Voort JC, Fay F, Calcagno C, et al. Nanobody-Facilitated Multiparametric PET/MRI Phenotyping of Atherosclerosis. JACC: Cardiovascular Imaging. 2018 2018/10/17/.
70. Varasteh Z, Hyafil F, Anizan N, Diallo D, Aid-Launais R, Mohanta S, et al. Targeting mannose receptor expression on macrophages in atherosclerotic plaques of apolipoprotein E-knockout mice using 111In-tilmanocept. EJNMMI Res. 2017 2017/5/03;7(1):40. [PubMed: 28470406]
71. Matter CM, Wyss MT, Meier P, Späth N, Lukowicz Tv, Lohmann C, et al. 18F-Choline Images Murine Atherosclerotic Plaques Ex Vivo. Arter Thromb Vasc Biol. 2006;26(3):584–9.
72. Laitinen IEK, Luoto P, Någren K, Marjamäki PM, Silvola JMU, Hellberg S, et al. Uptake of $^{11}$C-Choline in Mouse Atherosclerotic Plaques. J Nucl Med. 2010 5 1, 2010;51(5):798–802. [PubMed: 20395326]
73. Hellberg S, Silvola JMU, Kiugel M, Liljenbäck H, Metsälä O, Viljanen T, et al. Type 2 diabetes enhances arterial uptake of choline in atherosclerotic mice: an imaging study with positron emission tomography tracer 18F-fluoromethylcholine. Cardiovasc Diabetol. 2016 2016/2/06;15(1):26. [PubMed: 26852231]
74. Vöö S, Kwee RM, Sluimer JC, Schreuder FHBM, Wierts R, Bauwens M, et al. Imaging Intraplaque Inflammation in Carotid Atherosclerosis With 18F-Fluorocholine Positron Emission Tomography-Computed Tomography. Circ Cardiovasc Imaging. 2016;9(5):e004467.
75. Sanchez-Lopez E, Zhong Z, Stubelius A, Sweeney SR, Booshehri LM, Antonucci L, et al. Choline Uptake and Metabolism Modulate Macrophage IL-1β and IL-18 Production. Cell Metab. 2019 2019/6/04/;29(6):1350–62.e7. [PubMed: 30982734]
76. Bading JR, Shields AF. Imaging of Cell Proliferation: Status and Prospects. J Nucl Med. 2008 6 1, 2008;49(Suppl 2):64S–80S. [PubMed: 18523066]
77. Ye Y-X, Calcagno C, Binderup T, Courties G, Keliher EJ, Wojtkiewicz GR, et al. Imaging Macrophage and Hematopoietic Progenitor Proliferation in Atherosclerosis. Circ Res. 2015;117(10):835–45. [PubMed: 26394773]
78. McKinley ET, Ayers GD, Smith RA, Saleh SA, Zhao P, Washington MK, et al. Limits of [$^{18}$F]-FLT PET as a biomarker of proliferation in oncology. PLoS One. 2013;8(3):e58938. PubMed PMID: 23554961. Pubmed Central PMCID: PMC3598948. Epub 2013/04/05. eng.
79. Nahrendorf M, Zhang H, Hembrador S, Panizzi P, Sosnovik DE, Aikawa E, et al. Nanoparticle PET-CT Imaging of Macrophages in Inflammatory Atherosclerosis. Circulation. 2008;117(3):379–87. [PubMed: 18158358]
80. Majmudar MD, Yoo J, Keliher EJ, Truelove JJ, Iwamoto Y, Sena B, et al. Polymeric Nanoparticle PET/MR Imaging Allows Macrophage Detection in Atherosclerotic Plaques. Circ Res. 2013;112(5):755–61. [PubMed: 23300273]
81. Keliher EJ, Ye Y-X, Wojtkiewicz GR, Aguirre AD, Tricot B, Senders ML, et al. Polyglucose nanoparticles with renal elimination and macrophage avidity facilitate PET imaging in ischaemic heart disease. Nat Commun. 2017 2017/1/16;8(1):14064. [PubMed: 28091604]
82. Martz E Lymphocyte Function-Associated Antigen 1 (LFA-1). In: Delves PJ, editor. Encyclopedia of Immunology (Second Edition). Oxford: Elsevier; 1998. p. 1607–12.
83. Shaw SK, Ma S, Kim MB, Rao RM, Hartman CU, Froio RM, et al. Coordinated Redistribution of Leukocyte LFA-1 and Endothelial Cell ICAM-1 Accompany Neutrophil Transmigration. J Exp Med. 2004;200(12):1571–80. [PubMed: 15611287]
84. Watanabe T, Fan J. Atherosclerosis and inflammation: Mononuclear cell recruitment and adhesion molecules with reference to the implication of ICAM-1/LFA-1 pathway in atherogenesis. Int J Cardiol. 1998 1998/10/01/;66:S45–S53. [PubMed: 9951802]
85. Meester EJ, Krenning BJ, de Blois RH, Norenberg JP, de Jong M, Bernsen MR, et al. Imaging of atherosclerosis, targeting LFA-1 on inflammatory cells with 111In-DANBIRT. J Nucl Cardiol. 2018 2018/3/13.

86. Mota R, Campen MJ, Cuellar ME, Garver WS, Hesterman J, Qutaish M, et al. $^{111}$In-DANBIRT In Vivo Molecular Imaging of Inflammatory Cells in Atherosclerosis. Contrast Media Mol Imaging. 2018;2018:10.

87. Glaudemans AWJM, Bonanno E, Galli F, Zeebregts CJ, de Vries EFJ, Koole M, et al. In vivo and in vitro evidence that $^{99m}$Tc-HYNIC-interleukin-2 is able to detect T lymphocytes in vulnerable atherosclerotic plaques of the carotid artery. Eur J Nucl Med Mol Imaging. 2014 9 01;41(9):1710–9. [PubMed: 24737117]

88. Annovazzi A, Bonanno E, Arca M, D'Alessandria C, Marcoccia A, Spagnoli LG, et al. $^{99m}$Tc-interleukin-2 scintigraphy for the in vivo imaging of vulnerable atherosclerotic plaques. Eur J Nucl Med Mol Imaging. 2006 2 01;33(2):117–26. [PubMed: 16220305]

89. Di Gialleonardo V, Signore A, Glaudemans AWJM, Dierckx RAJO, De Vries EFJ. N-(4–18F-Fluorobenzoyl)Interleukin-2 for PET of Human-Activated T Lymphocytes. J Nucl Med. 2012 5 1, 2012;53(5):679–86. [PubMed: 22499614]

90. Fingleton B Matrix metalloproteinases as regulators of inflammatory processes. Biochimica et Biophysica Acta (BBA) - Molecular Cell Research. 2017 2017/11/01/;1864(11, Part A):2036–42. [PubMed: 28502592]

91. Hermann S, Starsichova A, Waschkau B, Kuhlmann M, Wenning C, Schober O, et al. Non-FDG imaging of atherosclerosis: Will imaging of MMPs assess plaque vulnerability? Journal of Nuclear Cardiology. 2012 6 01;19(3):609–17. [PubMed: 22477642]

92. Nathalie M, Aren van W, Rainer B, Ruth O, Christophe van de W, Rudi AJOD, et al. Probes for Non-invasive Matrix Metalloproteinase-targeted Imaging with PET and SPECT. Current Pharmaceutical Design. 2013;19(25):4647–72. [PubMed: 23339739]

93. Malm BJ, Sadeghi MM. Multi-modality molecular imaging of aortic aneurysms. J Nucl Cardiol. 2017 8;24(4):1239–45. PubMed PMID: 28447279. Epub 2017/04/28. eng. [PubMed: 28447279]

94. Toczek J, Ye Y, Gona K, Kim HY, Han J, Razavian M, et al. Preclinical Evaluation of RYM1, a Matrix Metalloproteinase-Targeted Tracer for Imaging Aneurysm. Journal of nuclear medicine : official publication, Society of Nuclear Medicine. 2017 8;58(8):1318–23. PubMed PMID: 28360209. Pubmed Central PMCID: PMC5537616. Epub 2017/04/01. eng.

95. Hu J, Van den Steen PE, Sang Q-XA, Opdenakker G. Matrix metalloproteinase inhibitors as therapy for inflammatory and vascular diseases. Nature Reviews Drug Discovery. 2007 2007/6/01;6(6):480–98. [PubMed: 17541420]

96. Levin M, Udi Y, Solomonov I, Sagi I. Next generation matrix metalloproteinase inhibitors — Novel strategies bring new prospects. Biochimica et Biophysica Acta (BBA) - Molecular Cell Research. 2017 2017/11/01/;1864(11, Part A):1927–39. [PubMed: 28636874]

97. Hakimzadeh N, Pinas VA, Molenaar G, de Waard V, Lutgens E, van Eck-Smit BLF, et al. Novel molecular imaging ligands targeting matrix metalloproteinases 2 and 9 for imaging of unstable atherosclerotic plaques. PLoS One. 2017;12(11):e0187767. PubMed PMID: 29190653. Pubmed Central PMCID: PMC5708805. Epub 2017/12/01. eng.

98. Toczek J, Bordenave T, Gona K, Kim HY, Beau F, Georgiadis D, et al. Novel Matrix Metalloproteinase 12 selective radiotracers for vascular molecular imaging. J Med Chem. 2019 10 11. PubMed PMID: 31603669. Epub 2019/10/12. eng.

99. Butsch V, Börgel F, Galla F, Schwegmann K, Hermann S, Schäfers M, et al. Design, (Radio)Synthesis, and in Vitro and in Vivo Evaluation of Highly Selective and Potent Matrix Metalloproteinase 12 (MMP-12) Inhibitors as Radiotracers for Positron Emission Tomography. Journal of Medicinal Chemistry. 2018 2018/5/10;61(9):4115–34. [PubMed: 29660282]

100. Hugenberg V, Wagner S, Kopka K, Schäfers M, Schuit RC, Windhorst AD, et al. Radiolabeled Selective Matrix Metalloproteinase 13 (MMP-13) Inhibitors: (Radio)Syntheses and in Vitro and First in Vivo Evaluation. Journal of Medicinal Chemistry. 2017 2017/1/12;60(1):307–21. [PubMed: 27981835]

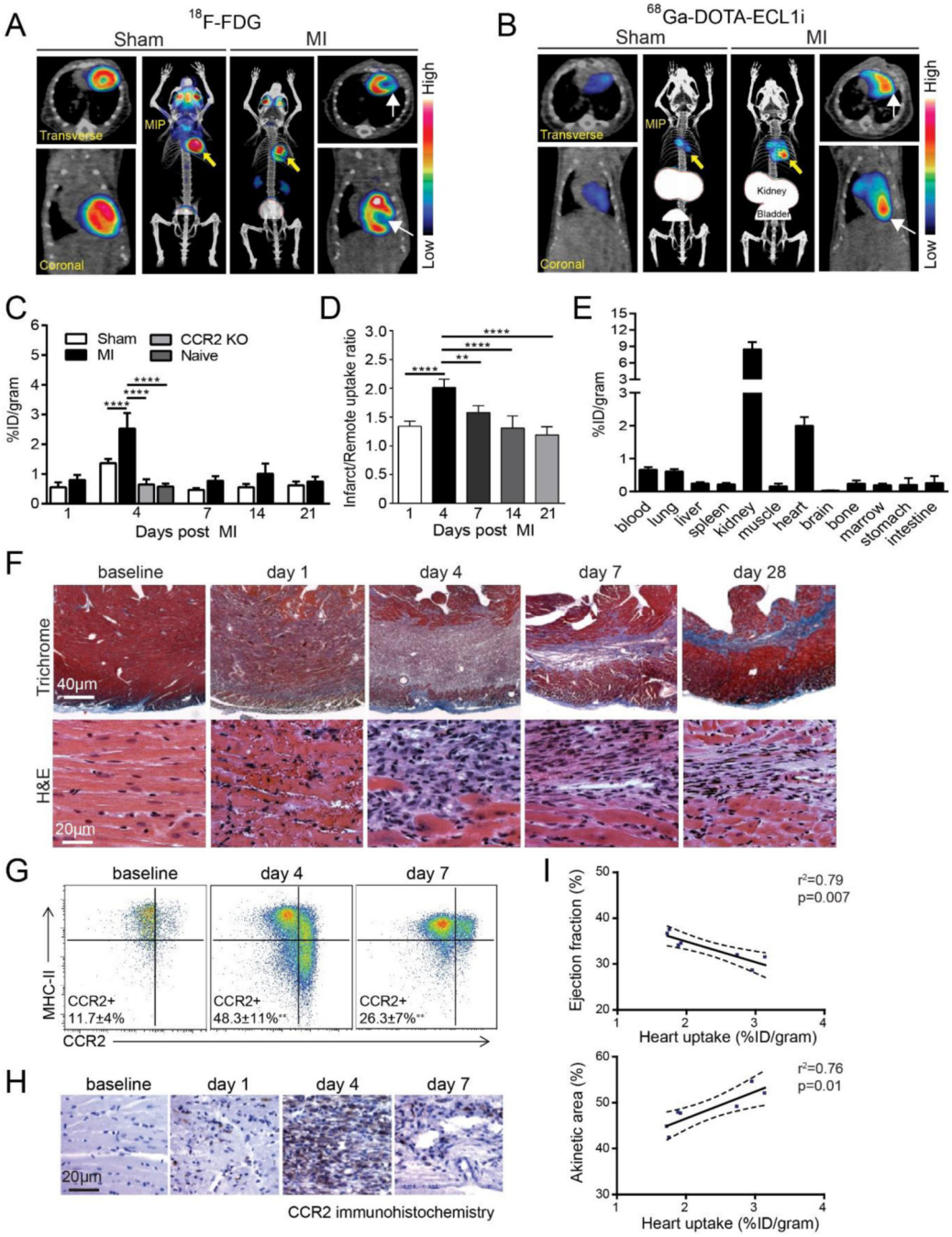


**Figure 1. Positron emission tomography (PET) of $^{68}$Ga-DOTA (1,4,7,10-tetraazacyclododecane-1,4,7,10-tetraacetic acid)-ECL1i (extracellular loop 1 inverso) in a mouse model of closed-chest ischemia-reperfusion injury.**

**A**, Representative $^{18}$F-fluorodeoxyglucose ($^{18}$F-FDG) PET/CT images obtained 5 d after 90 min of ischemia-reperfusion injury identifying the infarct region in mice that underwent ischemia-reperfusion injury (myocardial infarction [MI]) compared with sham controls. Transverse, coronal, and maximal-intensity projected (MIP) views are shown, and white arrows denote the infarct area. **B**, Representative $^{68}$Ga-DOTA-ECL1i PET/CT images showing regional accumulation of $^{68}$Ga-DOTA-ECL1i signal in the infarct and border zone

4 d after ischemia-reperfusion injury. Transverse, coronal, and MIP views are shown. Yellow arrow identifies tracer uptake in hearts that underwent ischemia-reperfusion injury compared with sham controls. White arrows denote the infarct area as determined by $^{18}$F-FDG imaging. **C**, Quantitative analysis of $^{68}$Ga-DOTA-ECL1i accumulation in the hearts of naive, sham, MI, and CCR2 (C-C chemokine receptor type 2) KO (knockout) mice that underwent ischemia-reperfusion injury at the indicated time points. n=4 to 5 per experimental group. **D**, Regional accumulation of $^{68}$Ga- DOTA-ECL1i uptake in the infarct and remote areas of sham and MI mice over the indicated time points. **E**, Biodistribution of $^{68}$Ga activity 4 d after ischemia-reperfusion injury measured 1 h post-intravenous injection (tail vein) of $^{68}$Ga-DOTA-ECL1i. n=5 per experimental group. **F**, Trichrome and hematoxylin and eosin (H&E) staining show the evolution of fibrosis (trichrome-blue, ×40 magnification) and cell infiltration (H&E, ×200 magnification) over time in the closed-chest ischemia-reperfusion injury model. Note the dense accumulation of cells within the infarct 4 d after ischemia-reperfusion injury. Representative images from 6 independent experiments. **G**, Flow cytometry analysis showing accumulation of CCR2+ monocytes (CCR2+MHCIIlow) and CCR2+ macrophages (CCR2+MHC-IIhigh) 4 d after ischemia-reperfusion injury and persistence of CCR2+ macrophages 7 d after ischemia reperfusion injury compared with sham controls. **H**, Immunostaining showing accumulation of CCR2+ cells (brown) in the infarct region peaking at day 4 after ischemia-reperfusion injury. **I**, Linear regression analyses showing the relationship between $^{68}$Ga-DOTA-ECL1i heart uptake measured on day 4 after ischemia-reperfusion injury and echocardiographic assessment of LV ejection fraction and akinetic area measured on day 28 after ischemiareperfusion injury. *$P$<0.05, **$P$<0.01, ***$P$<0.005, ****$P$<0.001. MHC indicates major histocompatibility complex. Reprinted with permission from reference [34]

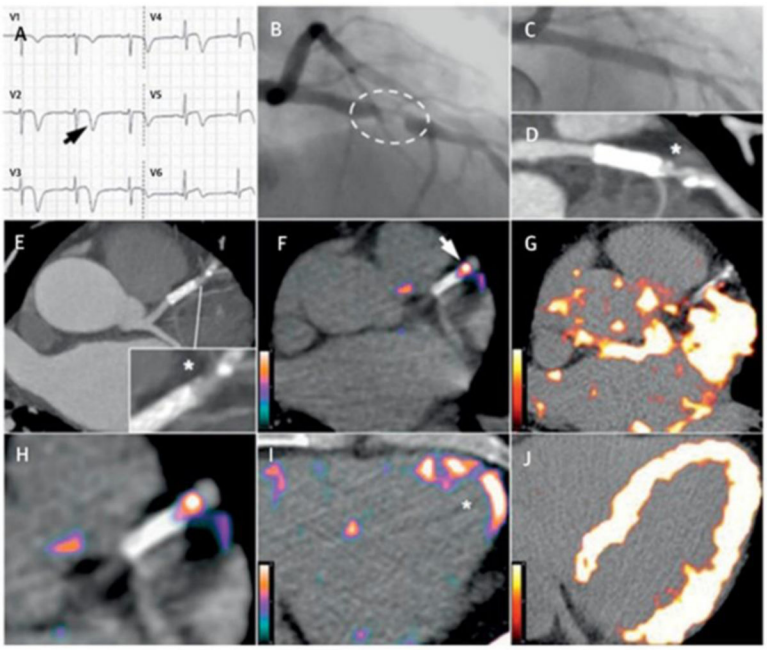


**Figure 2. Comparison between $^{68}$Ga-DOTATATE and $^{18}$F-FDG coronary PET inflammation imaging.**

Images from a 57-year old man with acute coronary syndrome who presented with deep anterolateral T-wave inversion **(arrow)** on electrocardiogram **(A)** and serum troponin-I concentration elevated at 4,650 ng/l (NR: <17 ng/l). Culprit left anterior descending artery stenosis **(dashed oval)** was identified by X-ray angiography **(B)**. After the patient underwent percutaneous coronary stenting **(C)**, residual coronary plaque **(*inset)** with high-risk morphology (low attenuation and spotty calcification) is evident on CT angiography **(D, E)**. Use of $^{68}$Ga-DOTATATE PET **(F, H, I)** clearly detected intense inflammation in this high-risk atherosclerotic plaque/distal portion of the stented culprit lesion **(arrow)** and recently infarcted myocardium **(*)**. In contrast, using $^{18}$F-FDG PET **(G, J)**, myocardial spillover completely obscures the coronary arteries. CT = computed tomography; $^{18}$F-FDG = fluorine-18-labeled fluorodeoxyglucose; $^{68}$Ga-DOTATATE = gallium-68-labeled DOTATATE; PET = positron emission tomography. Adapted with permission from reference [13]

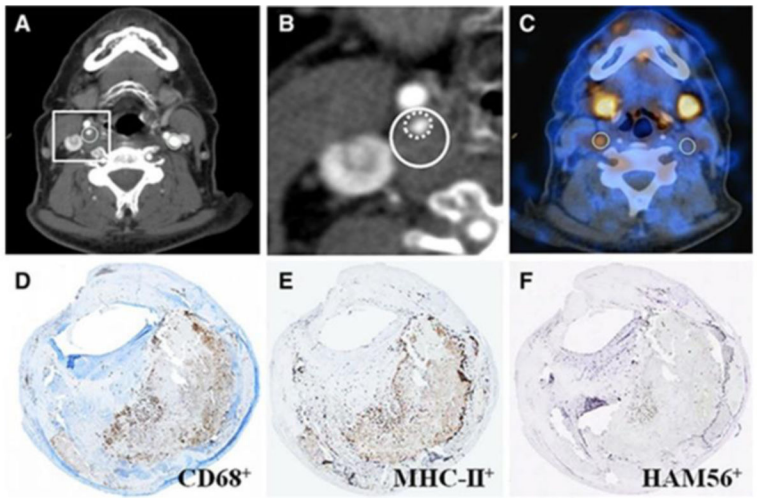


**Figure 3.**

Representative $^{18}$F-fluorocholine positron emission tomography-computed tomography ($^{18}$F-FCH PET-CT) images and corresponding histology of a symptomatic and contralateral asymptomatic carotid plaque of a 67-year-old patient who experienced right-sided stroke 12 days before PET-CT imaging. **A**, Diagnostic contrast-enhanced CT shows a significant stenosis in the right internal carotid artery because of a soft plaque, whereas no atherosclerotic plaque can be seen on the contralateral internal carotid artery. Regions of interest (ROI, white outlining) drawn around the outer border of the vessel walls were placed along the right carotid stenosis and along the contralateral carotid artery, respectively. **B**, CT, inset on the symptomatic plaque. **C**, The fused PET-CT image denotes a focal area of high $^{18}$F-FCH uptake in the ROI drawn onto the right symptomatic carotid plaque, whereas there is no visible 18F-FCH uptake in the left asymptomatic carotid plaque. The activity recorded for both symptomatic and contralateral asymptomatic carotid arteries were corrected for venous blood background activity in the jugular veins, resulting in a maximum target-to-background ratio of 2.46 and 1.18, respectively. Corresponding immunohistochemistry sections indicating CD68+ (**D**), MHC-II+ (**E**), and HAM56+ (**F**) cells (all in brown). MHC-II indicates major histopathology complex class-II; HAM56, human alveolar macrophage marker-56. Reprinted with permission from reference [74]

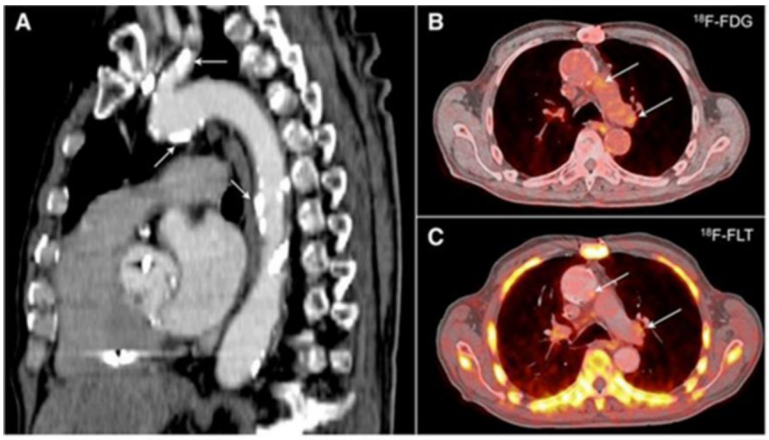


**Figure 4.**

$^{18}$F-FLT and $^{18}$F-FDG positron emission tomography–computed tomography (PET-CT) in humans with atherosclerosis. **A**, Sagittal image revealing extensive calcification in the aorta and carotid artery (arrows). $^{18}$F-FDG (**B**) and $^{18}$F-FLT (**C**) images demonstrate uptake of the PET tracers in the vessel wall of the aortic arch (arrows). Adapted with permission from reference [77]

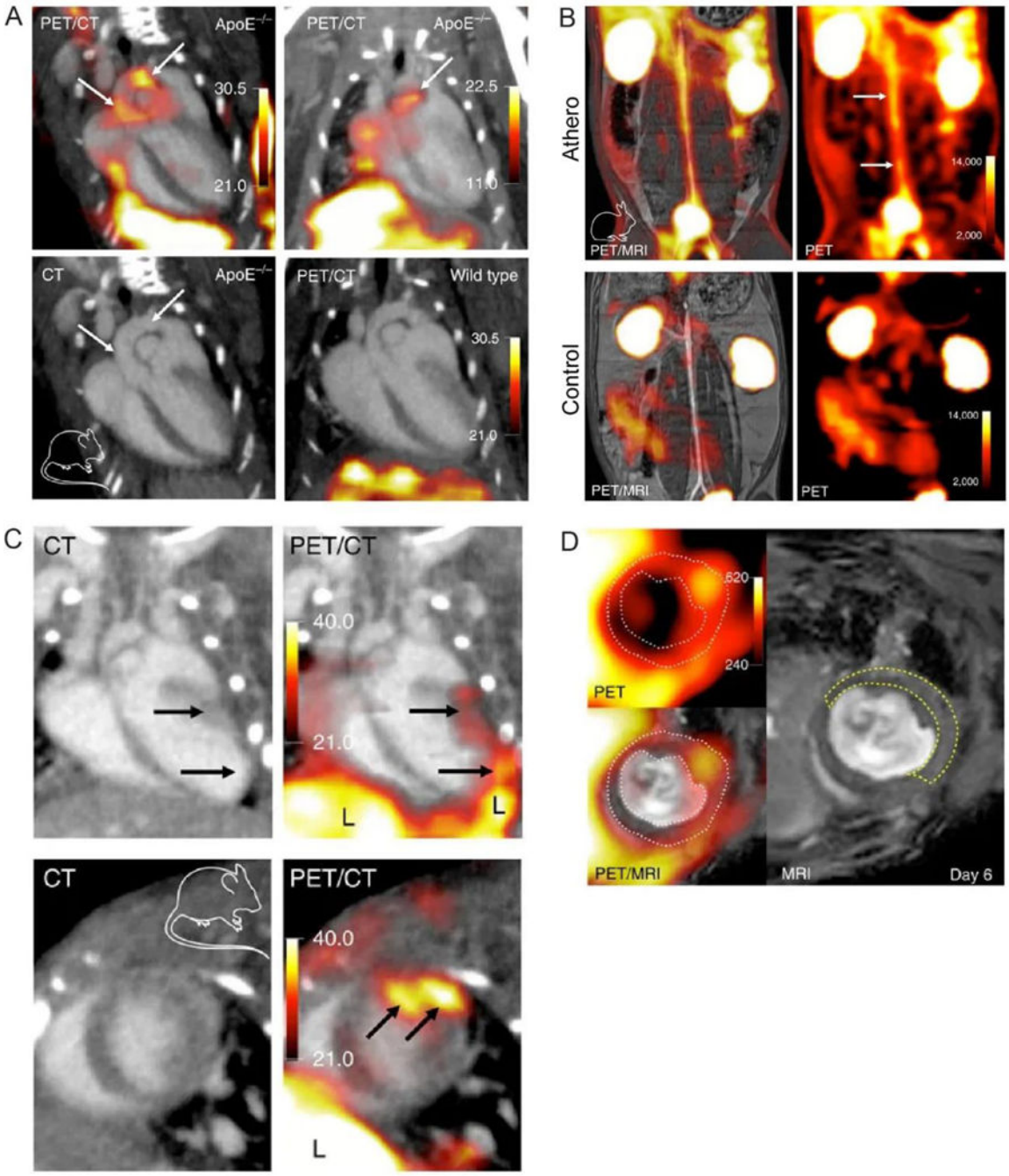


**Figure 5. Applications of $^{18}$F-Macroflor.**

PET imaging of aortic plaques in atherosclerotic mice (**A**) and rabbits (**B**). PET imaging of mice with acute myocardial infarction at day 6 post MI (**C** and **D**). White dotted line on PET/MRI outlines myocardium. Yellow dashed line on MRI outlines the infarct identified by gadolinium enhancement and wall motion abnormality in cine loops. Adapted with permission from reference [81]